



OPEN

DATA DESCRIPTOR

Chromosome-level genome assembly of the caenogastropod snail *Rapana venosa*

Hao Song^{1,2,3,5}, Zhuoqing Li^{1,3,5}, Meijie Yang^{1,2,3,5}, Pu Shi^{1,3,5}, Zhenglin Yu⁴, Zhi Hu^{1,3}, Cong Zhou^{1,3}, Pengpeng Hu^{1,3} & Tao Zhang^{1,2,3}✉

The carnivorous gastropod *Rapana venosa* (Valenciennes, 1846) is one of the most notorious ecological invaders worldwide. Here, we present the first high-quality chromosome-scale reference *R. venosa* genome obtained via PacBio sequencing, Illumina paired-end sequencing, and high-throughput chromosome conformation capture scaffolding. The assembled genome has a size of 2.30Gb, with a scaffold N50 length of 64.63 Mb, and is anchored to 35 chromosomes. It contains 29,649 protein-coding genes, 77.22% of which were functionally annotated. Given its high heterozygosity (1.41%) and large proportion of repeat sequences (57.72%), it is one of the most complex genome assemblies. This chromosome-level genome assembly of *R. venosa* is an important resource for understanding molluscan evolutionary adaptation and provides a genetic basis for its biological invasion control.

Background & Summary

Caenogastropoda is an extraordinarily large and diverse group containing thousands of described species and comprising ~60% of extant gastropod species¹. These snails are extremely diverse in morphology, diet, and habitat and inhabit marine, terrestrial, and freshwater environments in the wild^{2,3}. To date, only two chromosome-level genomes of this clade have been published^{4,5}, which limits our understanding of the internal phylogeny and evolutionary adaptation of this important clade.

Rapana venosa (Valenciennes, 1846) is a common marine carnivorous snail in the Caenogastropoda. It is native to the coasts of the Bohai, East, and Yellow Seas in China, the northern Korean peninsula, the far east of Russia, and northern Japan⁶, and is an economically important species in China⁷. Via global transport, *R. venosa* has unintentionally been introduced into the Rio de la Plata between Argentina and Uruguay, Chesapeake Bay, Quiberon Bay in France, and the coastal waters of the Netherlands, as an invasive species^{8–11}. Its successful establishment in these areas is based on its strong ecological fitness, involving high fecundity, easy dispersal as planktonic larvae, rapid growth rate, early sexual maturity, and broad tolerance to oxygen depletion, salinity, temperature, and water pollution¹². In the Chesapeake Bay region, *R. venosa* has very different prey and predation strategies from the native gastropod, *Urosalpinx cinerea*, and therefore disrupts the local trophic structure and attenuation of native shellfish resources¹³. As *R. venosa* feeds on economically valuable bivalves, such as oysters, mussels, and clams, it has also caused severe economic losses in the Black Sea area¹⁴. The economic importance in Asian countries and global ecological invasiveness of this species has led to extensive studies on its developmental mechanism and the genetic basis of its environmental adaptation^{15–17}. However, such studies are hampered by the lack of related genomic resources.

In this study, we used short reads generated by an Illumina platform, long reads generated by PacBio sequencing, and high-throughput chromosomal conformation capture (Hi-C) analysis to construct a high-quality *R. venosa* reference genome at the chromosomal level (Fig. 1). The genome sequences were assembled into 17,949 contigs, with a contig N50 length of 434.10 kb and a total length of 2.30 Gb. Chromosome scaffolding resulted in 5,242 sequences corresponding to 35 chromosomes. The largest 35 chromosome scale scaffolds are in total

¹CAS Key Laboratory of Marine Ecology and Environmental Sciences, Institute of Oceanology, Chinese Academy of Sciences, Qingdao, 266071, China. ²Laboratory for Marine Ecology and Environmental Science, Qingdao National Laboratory for Marine Science and Technology, Qingdao, 266237, China. ³University of Chinese Academy of Sciences, Beijing, 100049, China. ⁴Research and Development Center for Efficient Utilization of Coastal Bioresources, Yantai Institute of Coastal Zone Research, Chinese Academy of Sciences, Yantai, 264003, China. ⁵These authors contributed equally: Hao Song, Zhuoqing Li, Meijie Yang, Pu Shi. ✉e-mail: tzhang@qdio.ac.cn

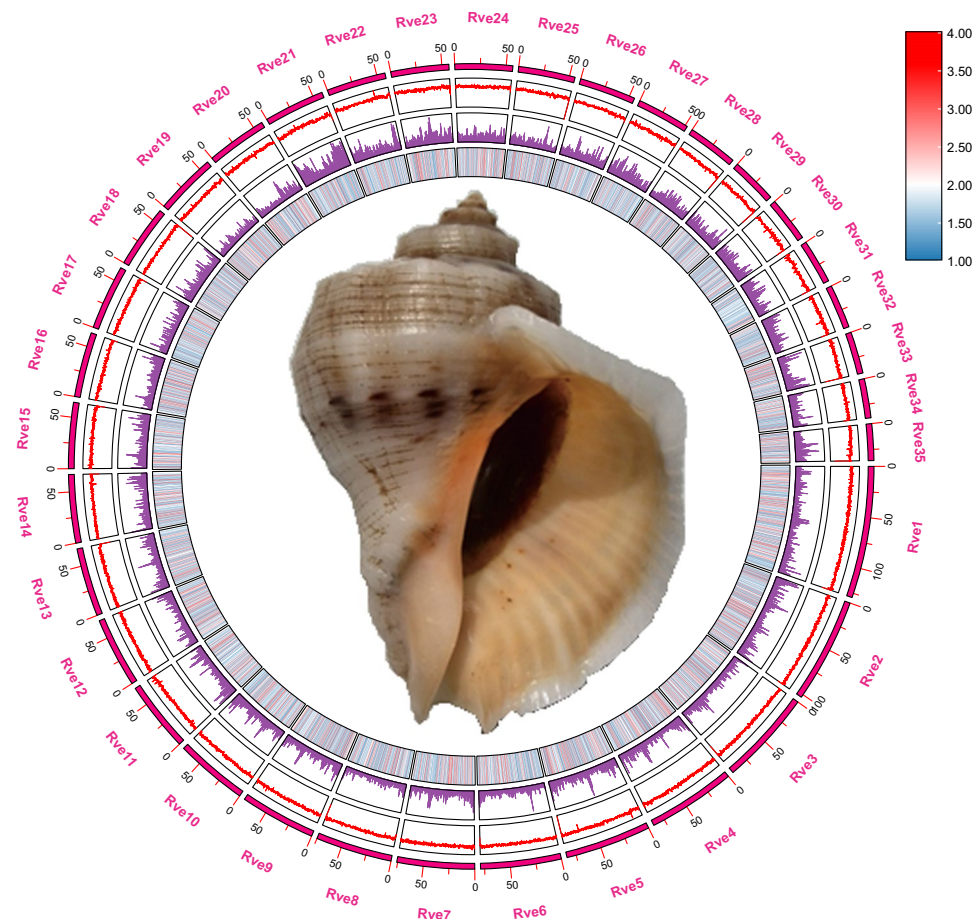


Fig. 1 Characterization of assembled *R. venosa* genome. From inner to outer layers: photograph of *R. venosa*, gene abundance, repeat element abundance, GC rate, and chromosome-level scaffolds at scale.

2.25 Gb long, which corresponds to 97.88% of the total contig length. Using *de novo* and homolog-based strategies, 29,649 protein-coding genes were revealed by gene annotation, 77.22% of which were annotated in the publicly available NCBI RefSeq non-redundant protein, KEGG, TrEMBL, Swissprot, and InterPro databases. The *R. venosa* genome assembly has a high heterozygosity of 1.41% and a large proportion of repeat sequences (57.72%) and, therefore, is one of the most complex genome assemblies. Phylogenetic analysis indicated that *R. venosa* speciated from the common ancestor of *Conus consors* approximately 124.4 mya (78.3–177.5 mya).

Methods

Sample collection and sequencing. Living specimens of *R. venosa* were collected from Laizhou Bay, China. We extracted genomic DNA from *R. venosa* muscle samples using a QIAGEN DNeasy Kit (QIAGEN, Shanghai, China) as per the product manual. We used electrophoresis on a 1% agarose gel to examine the quality of the isolated genomic DNA. To ensure the DNA samples met the sequencing requirements, we used a Qubit instrument to quantify the concentration and 23.2 ng/μL DNA was obtained. Then, the genomic DNA was purified and concentrated by AMPure PB magnetic beads. The processed genomic DNA was further applied to prepare a single-molecule real-time sequencing library using the SMRTbell Template Prep Kit 2.0 (Pacific Biosciences, Menlo Park, CA, USA)¹⁸. The library was sequenced using the Pacific Biosciences Sequel II in continuous long-read (CLR) mode following the manufacturer's instructions. As a result, 3 SMRT cells were sequenced, and we obtained a total of 256.49 Gb PacBio reads. The N50 and N90 lengths of the reads were 434.10 kb and 58.92 kb, respectively. Based on the protocol, we constructed the Illumina short-insert (350 bp) library. Paired-end sequencing was performed on the Illumina Novaseq 6000 platform (Illumina, Inc., San Diego, CA, USA) and a total of 153.00 Gb reads were obtained. For the Hi-C sequencing, fresh muscle was fixed in 1% formaldehyde and the fixation was terminated with 0.2 M glycine. In accordance with the protocol¹⁹, we prepared the Hi-C library and then sequenced on an Illumina NovaSeq 6000 sequencing platform¹⁹.

Genome assembly. *R. venosa* genome assembly was challenging because of the extremely high percentages of sequence repeats (57.72%) and heterozygosity (1.41%). We tried different genome-assembly strategies and ultimately selected that with the highest continuity and accuracy (Table 1). In total, 256.49 Gb of PacBio long-read data was used for *de novo* genome assembly using wtdbg v 2.4²⁰, which resulted in 17,949 contigs and a contig N50 length of 434.10 Kb. We then used Pilon v 1.23²¹ to polish the assembled genome with the Illumina short

Method	Contig length	Contig N50	BUSCO
wtdbg2.4 + pilon + purge_haplotigs_full	2,295,076,713	434,100	90.60%
wtdbg2.0 + purge_haplotigs	3,815,562,603	944,770	83.20%
wtdbg2.4 + pilon + pilon	2,293,399,401	434,579	89.80%
wtdbg2.4 + pilon	3,105,793,653	239,999	90.10%
wtdbg2.0 + pilon	3,135,630,390	223,757	88.60%
wtdbg2.0	3,135,165,531	233,566	84.60%
wtdbg2.4	3,105,429,266	239,655	85.10%
wtdbg2.6	3,202,933,435	222,469	85.30%

Table 1. Comparison of effects of different genome assembly schemes.

Genome Name	Before Hi-C	After Hi-C
Seq Type	Contig	Scaffold
Total Number	17,949	5,242
Total Length (bp)	2,293,821,241	2,300,182,741
N50 (bp)	434,100	64,632,560
N90 (bp)	434,100	43,368,723
Max Length (bp)	5,188,507	129,259,876
Min Length (bp)	2,089	2,089
Gap Length (bp)	0	6,361,500
GC Content (%)	42.38	42.38

Table 2. Assembly statistics of *R. venosa* genome.

	Gene number	Percentage
Complete BUSCOs (C)	886	90.6%
Complete and single-copy BUSCOs (S)	832	85.1%
Complete and duplicated BUSCOs (D)	54	5.5%
Fragmented BUSCOs (F)	18	1.8%
Missing BUSCOs (M)	74	7.6%
Total BUSCO groups searched	978	100%

Table 3. Statistical result of BUSCO evaluation results of genome assembly.

reads from the same individual. Purge Haplotigs software was used to remove redundancy from the assembled genome, obtaining a 2,293.82 Mb long assembly (Table 2). The total gene space was 38.3 Mb and the mean exon number per mRNA was about six. In our previous genome survey analysis, the estimated genome size of *R. venosa* was 2.20 Gb with 67.04% sequence repeats using a *k*-mer analysis, quite near to the assembly in this study²². The genome assembly size of *R. venosa* is substantially larger than those of some closely related mollusc species, such as *Crassostrea gigas* (557.74 Mb)²³, *Biomphalaria glabrata* (916.38 Mb)²⁴, *Pomacea canaliculata* (440.07 Mb)²⁵, and *Achatina immaculata* (1.65 Gb)²⁶, similar to those of *Octopus bimaculoides* (2.40 Gb)²⁷ and *Conus consors* (2.05 Gb)⁵, and smaller than that of *Conus bullatus* (3.43 Gb)⁴. Benchmarking Universal Single-Copy Orthologs (BUSCO) v 5.4.6²⁸ was used to evaluate the completeness and quality of the *R. venosa* genome assembly against the metazoa_odb10 database. Of the 978 BUSCO orthologous groups, 886 (90.6%) were identified as complete in the assembled genome (Table 3). This assembly was even better than the recently published genome of another Neogastropoda member, *C. bullatus*, with a contig N50 length of 171.48 kb and a BUSCO (v 5.4.6) value of 89.8%⁴. The GC content of the *R. Rapana* genome assembly is 42.38%.

Chromosomal-level genome scaffolding with Hi-C data. In total, 4991.96 million read pairs raw data were obtained from the Hi-C sequencing. We conducted quality control, sorting, and duplication removal using HiC-Pro v. 2.8.0²⁹. Using the Burrows-Wheeler Aligner (v. 0.7.10-r789)³⁰, 63.86% of the clean data were aligned to the draft genome assembly. Here, after using Juicer v1.5^{31,32} and 3D-DNA v170123³³ to infer order and orientation, 97.88% of the contigs could be placed into 35 scaffolds (chromosomes), with their lengths ranging from 35.91 Mb to 129.26 Mb (Fig. 1, Table 4). After Hi-C scaffolding, the final *Rapana* genome assembly had a size of 2,251.40 Mb and a scaffold N50 of 64.63 Mb (Table 2). A chromatin contact matrix was manually curated in Juicebox v1.5³⁴ and the 35 scaffolds are clearly distinguishable in the heatmap in Fig. 2; the interaction signal around the diagonal is strongly apparent.

Chromosome ID	Length (bp)	Percentage
1	129,259,876	5.62
2	102,937,426	4.48
3	93,021,499	4.04
4	86,596,267	3.76
5	84,105,318	3.66
6	78,962,513	3.43
7	75,945,163	3.30
8	75,018,702	3.26
9	74,270,578	3.23
10	71,298,014	3.10
11	68,941,643	3.00
12	68,591,446	2.98
13	67,222,234	2.92
14	66,967,177	2.91
15	64,632,560	2.81
16	63,771,600	2.77
17	63,638,393	2.77
18	61,408,853	2.67
19	60,192,790	2.62
20	59,395,429	2.58
21	59,572,819	2.59
22	58,189,201	2.53
23	56,867,690	2.47
24	56,540,346	2.46
25	55,602,779	2.42
26	55,382,934	2.41
27	52,294,145	2.27
28	49,418,871	2.15
29	45,417,075	1.97
30	44,063,510	1.92
31	43,368,723	1.89
32	43,032,484	1.87
33	41,114,260	1.79
34	38,441,582	1.67
35	35,913,348	1.56
Total	2,251,397,248	97.88
Unplaced	48,785,493	2.12

Table 4. Statistics of *R. venosa* genome sequence length (chromosome level).

Repeat sequences and genome annotation. We used *ab initio* prediction and homology comparison to annotate the repetitive *R. venosa* genomic elements. For the *ab initio* repeat annotation, we used RepeatModeler v. 1.0.9³⁵, LTR_FINDER v. 1.0.7³⁶, and RepeatScout v. 1.0.7³⁷ to build a *de novo* repetitive element database. We used RepeatMasker v. 4.0.7³⁸ to annotate the repeat elements in the database. We used RepeatMasker v. 4.0.7 and RepeatProteinMask v. 4.0.7 to identify the known repeat element types via searching the Repbase v. 20181026³⁹. In addition, Tandem Repeats Finder (TRF v. 4.09)⁴⁰ was used to annotate tandem repeats, identifying 1327.65 Mb of repetitive sequences, representing 57.72% of the assembled genome. This proportion is substantially higher than in closely related species, such as *Lottia gigantea* (10.39%)⁴¹, *Aplysia californica* (21.80%)⁴², *P. canaliculata* (11.27%)²⁵, and *C. bullatus* (38.56%)⁴. Among the repeat sequences, long interspersed nuclear elements were dominant (911.70 Mb, 39.636% of the assembled genome), and short interspersed nuclear elements were the rarest (6.09 Mb, 0.27%) (Table 5).

Candidate non-coding RNAs were annotated as follows. Ribosomal and transfer RNAs were predicted through BLASTN v. 2.2.28⁴³ and tRNAscan-SE v. 1.4⁴⁴ (www.lowelab.ucsc.edu/tRNAscan-SE/), respectively. We thus annotated 165 rRNA and 3,241 tRNA genes (e-value: $1e^{-10}$). We searched against the Rfam database using Infernal v. 1.1.2⁴⁵ (<http://infernal.janelia.org/>) and identified 76 micro and 103 small nuclear RNAs.

We applied *de novo*, homology-based, and transcriptomic strategies to annotate the protein coding genes in the *R. venosa* genome. For the *de novo* prediction, Augustus v. 3.2.3⁴⁶, pre-trained using the transcripts assembled from the RNA-seq of *R. venosa*, was employed to predict the coding regions on the repeat-masked assembly. The optimal parameters were obtained after the model training. For the homology-based prediction, we first downloaded the protein sequences of closely related molluscan species, including *L. gigantea*, *C. consors*,

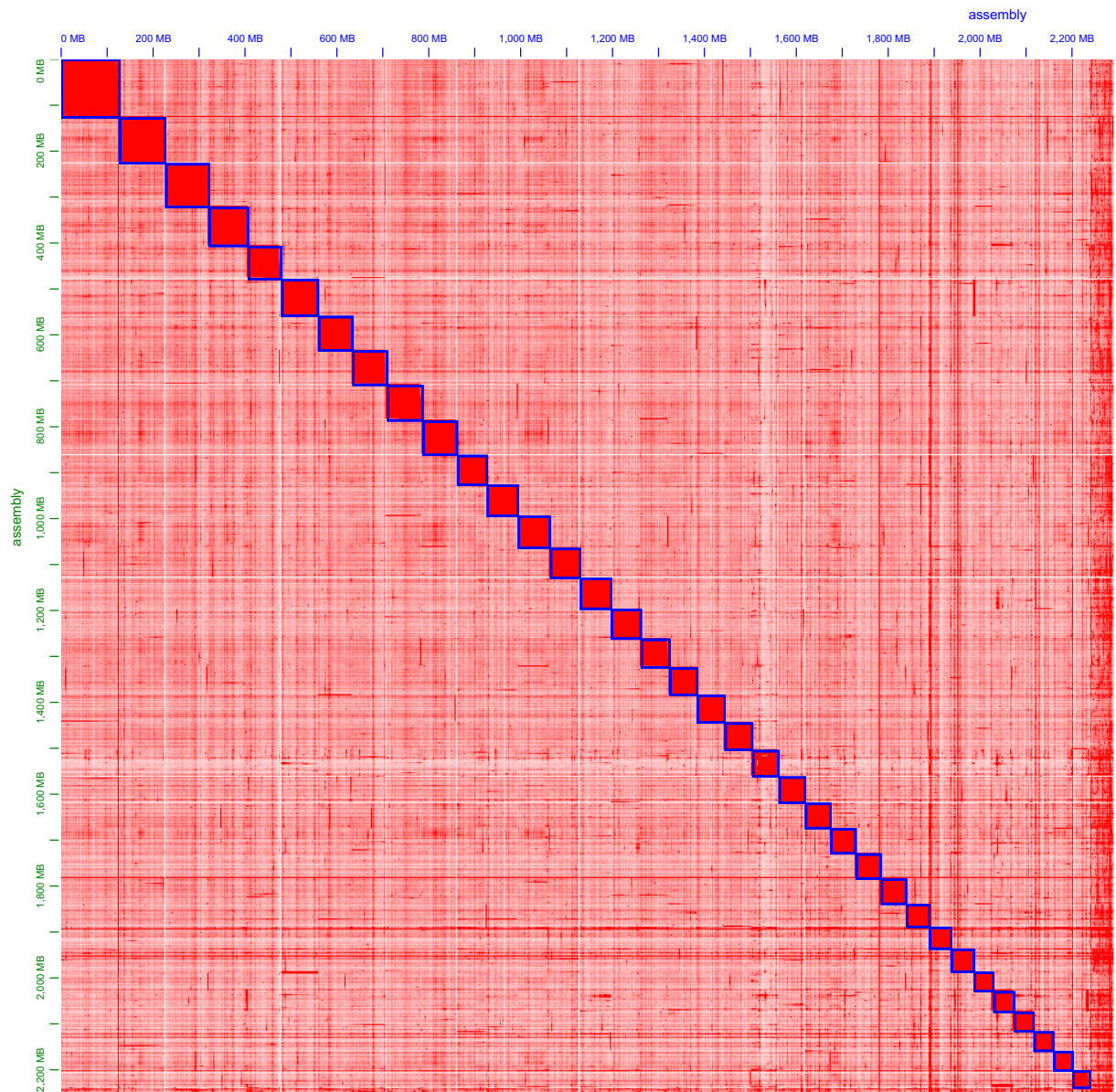


Fig. 2 Hi-C assembly of chromosome interactive heat map. Abscissa and ordinate represent order of each bin on corresponding chromosome group. Color block illuminates intensity of interaction from white (low) to red (high).

Type	Rebase TEs		Protein TEs		Denovo TEs		Combined TEs	
	Length(bp)	% of genome	Length(bp)	% of genome	Length(bp)	% of genome	Length(bp)	% of genome
DNA	434,449,483	18.888	785,583	0.034	402,828,966	17.513	674,041,712	29.304
LINE	177,491,372	7.716	137,364,314	5.972	822,399,881	35.754	911,702,236	39.636
SINE	1,911,991	0.083	0	0	4,221,194	0.184	6,094,063	0.265
LTR	101,206,291	4.4	2,408,799	0.105	552,520,316	24.021	606,176,386	26.353
Other	47,955	0.002	0	0	0	0	47,955	0.002
Unknown	0	0	0	0	3,681,471	0.16	3,681,471	0.16
Total	566,012,533	24.607	140,548,746	6.11	1,296,949,871	56.385	1,327,648,628	57.719

Table 5. Classification of repeat elements in the *R. venosa* genome.

P. canaliculata, *A. californica*, *A. immaculata*, *Elysia chlorotica*, *B. glabrata*, *C. gigas*, *Octopus vulgaris*, and *Haliothis rubra* from the NCBI database. These protein sequences were aligned against the genome assembly using BLAT

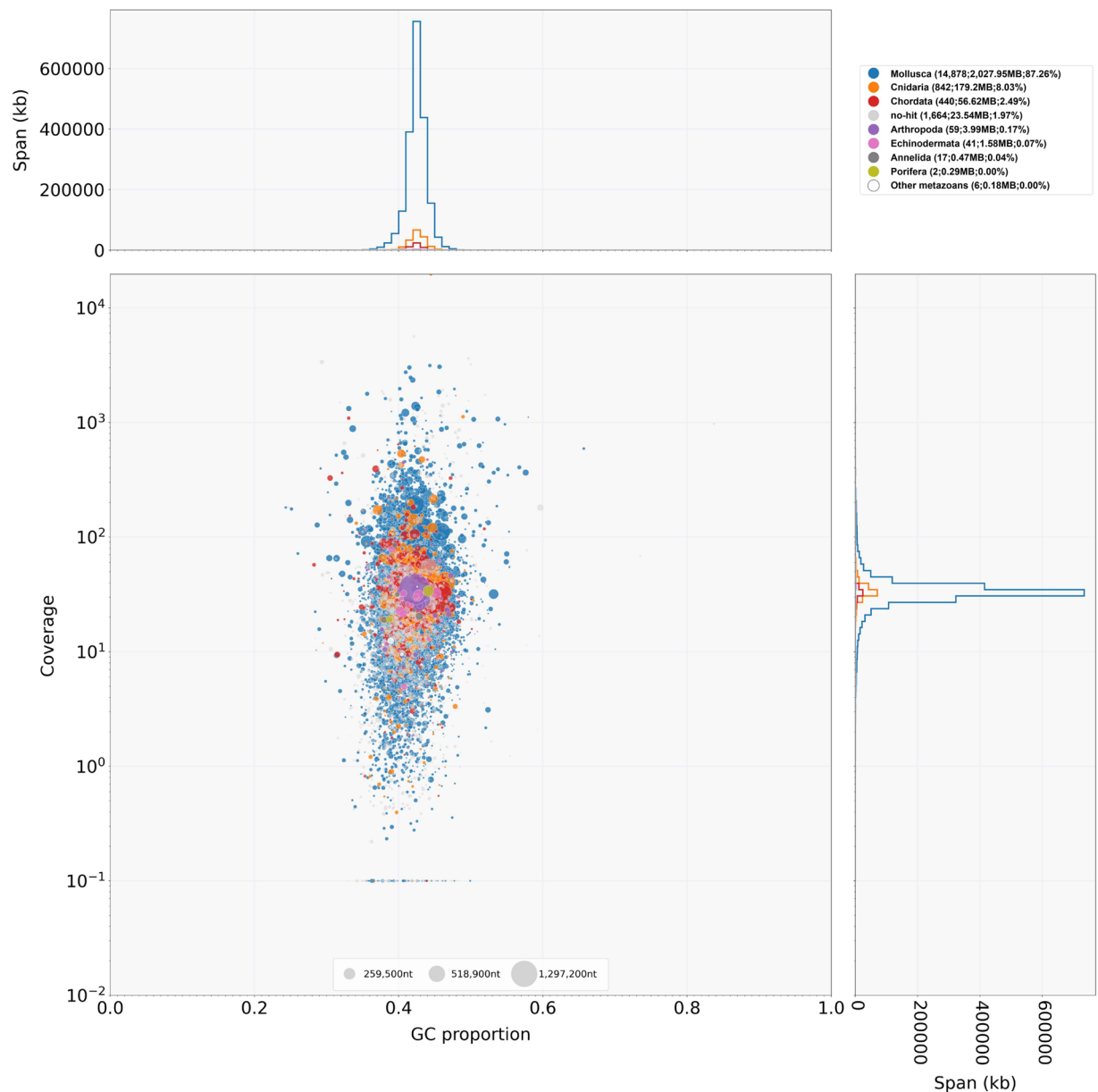


Fig. 3 Taxon-annotated GC-coverage plot (BlobPlot) of the contigs used for *R. venosa* genome assembly. Each circle represents a contig sequence, plotted relative to its base coverage and GC proportion. Circle diameter is proportional the size of the contig it represents. Circles are colored according to their assigned taxon at the phylum level (see legend). Histograms show the distribution of the total assembly length along each axis.

v. 35⁴⁷ with an e-value threshold of $1e^{-5}$. Then, we used GeneWise v. 2.4.1⁴⁸ to align the matching proteins to the homologous genomic sequences to accurately splice the alignments. For the transcriptomic prediction, Hisat v. 2.0.4⁴⁹ and Stringtie v. 1.2.3⁵⁰ were used for assembly based on the reference transcripts, and TransDecoder v. 5.5.0 (https://15k.nal.usda.gov/Tigriopus_californicus) was used for gene prediction. Finally, all results were merged to form a consensus gene set using GLEAN⁵¹, and 29,649 protein-coding genes were predicted. To functionally annotate the protein-coding genes, we searched public biological functional databases (SwissProt, InterPro, KEGG, and TrEMBL) for their sequences using BLASTX v. 2.2.28⁴³ and BLASTN v. 2.2.28⁴³ with an e-value threshold of $1e^{-5}$; 22,894 genes (77.22%) were annotated in at least one public database.

Data Records

The raw Illumina, PacBio, and Hi-C sequencing data are deposited in the NCBI SRA database under the accession numbers SRR22889214⁵², SRR23517974⁵³, SRR23501451⁵⁴, SRR23501452⁵⁵, SRR23501453⁵⁶, and SRR23501454⁵⁷, respectively. The genome assembly has been deposited in the NCBI SRA database under the accession number JAQIHA000000000⁵⁸. The genome annotations are available from the Figshare repository⁵⁹.

	Result
Read mapping rate (%)	99.30
Genome average sequencing depth (×)	27.25
Coverage of genome (%)	78.51
Coverage of genome > 4 × (%)	68.79
Coverage of genome > 10 × (%)	59.70
Coverage of genome > 20 × (%)	48.09

Table 6. Statistical results of short read alignment.

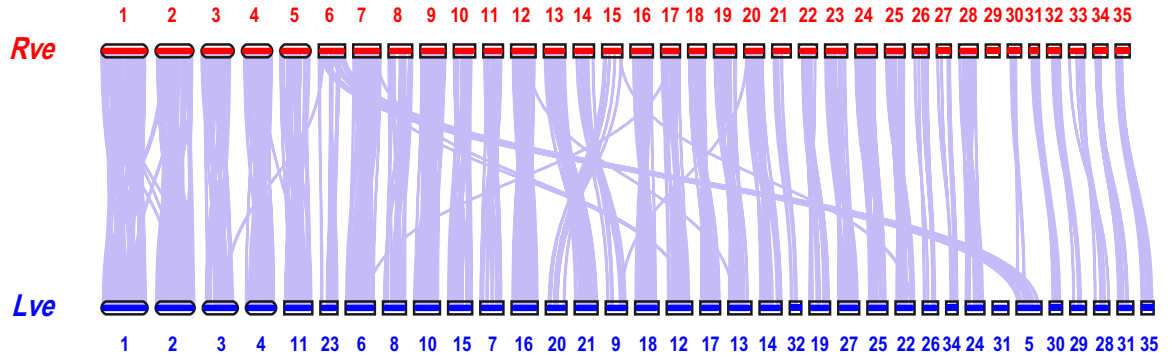


Fig. 4 Genomic synteny between *R. venosa* and *L. ventricosus*.

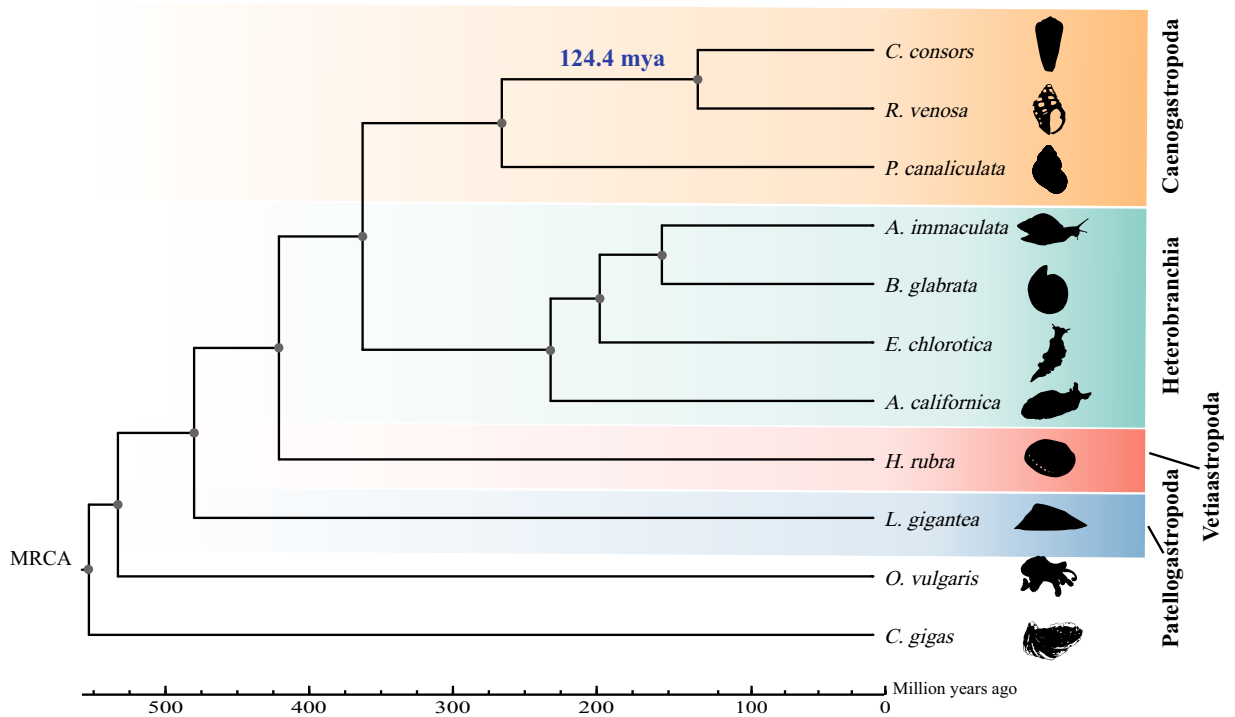


Fig. 5 Phylogenetic analysis of *R. venosa* and 10 other species.

Technical Validation

Evaluating genome assembly and annotation completeness. The assembled *R. venosa* genome size is 2.30 Gb with a scaffold N50 of 64.63 Mb (Fig. 1), close to the estimated size in previous studies²². Using blobtools v. 1.1.1⁶⁰, we created a blobplot to evaluate possible contamination of the contigs used for genome assembly (Fig. 3). As a result, we determined that 87.26% of the contigs had BLAST hits to mollusca. The remaining 12.74% of the contigs were categorized as follows: 8.03% as cnidaria, 2.49% as chordata, 0.17% as arthropoda, 0.07% as

echinodermata, 0.04% as annelida, and 1.97% did not match any taxonomic group. These results suggest that the contigs used for *R. venosa* genome assembly were not contaminated with microorganisms. For the quality assessment of the genome assembly, an 90.6% completeness of BUSCO was obtained. The protein-coding sequence possessed an 89.1% completeness of BUSCO. These results suggest a high-quality *R. venosa* genome assembly considering its high heterozygosity and repeat content. The Illumina short reads were mapped to the assembled genome using BWA v. 0.7.10 to evaluate the completeness of the genome assembly³⁰. As shown in the Tables 6, 99.30% of the reads could be mapped, covering 78.51% of the assembled genome (Table 6). The Hi-C heatmap shows a well-organized interaction pattern within the chromosomal region (Fig. 2), and assembly resulted in 35 chromosome-level scaffolds, in line with previously published karyotyping⁴⁸. Taken together, these confidently confirm the accuracy of the chromosome scaffolding.

Collinearity analysis and phylogenetic analysis. Collinearity analysis of chromosomes between *R. venosa* and another Caenogastropoda species *Lautoconus ventricosus*⁶¹ was conducted with LASTZ v. 1.02.00⁶². As shown in Fig. 4, almost 35 chromosome-level scaffolds of *R. venosa* displayed high homology with the corresponding chromosomes of *L. ventricosus*, which is suggestive of high quality sequencing and assembly and also make phylogenetic analysis more reliable. For phylogenetic analysis, we conducted pairwise sequence comparisons to predict orthologous genes. First, BLASTP v. 2.2.28 with an e-value cutoff of $1e^{-7}$ was used to compare the protein sequences of all species. Then, TreeFam v. 9⁶³ was applied to cluster all genes. The species used in the gene family clustering analysis were *R. venosa*, *H. rubra*, *L. gigantea*, *C. consors*, *P. canaliculata*, *A. californica*, *A. immaculata*, *E. chlorotica*, *B. glabrata*, *C. gigas*, and *O. vulgaris*.

Phylogenetic trees were constructed based on single-copy orthologous gene families. Based on the alignment results of the orthologous protein sequences in MUSCLE v. 5.1⁶⁴, the corresponding coding regions of these protein sequences were selected. We extracted the fourfold degenerate synonymous sites of each alignment and concatenated them to form an individual supergene for each species. We used the supergene alignments to perform a maximum likelihood tree using PhyML v. 2.4.4⁶⁵, MrBayes v. 3.2.6, and RAxML v. 8.2.12⁶⁶, respectively. Finally, the tree was visualized using Figtree (Fig. 4a). The phylogenetic tree shows that *R. venosa* and *C. consors* cluster into one clade, and the positions of the other clades are consistent with previously findings²⁶. MCMCtree⁶⁷ in PAML v. 4.4b⁶⁸, with a correlated molecular clock and HKY85 substitution model, was selected to estimate the divergence times between species. Five calibration nodes were used: *C. gigas* and *O. vulgaris* 532–582 mya, *H. rubra* and *P. canaliculata* 401–507 mya, *L. gigantea* and *A. californica* 401–507 mya, *R. venosa* and *P. canaliculata* 155–508 mya, and *E. chlorotica* and *C. consors* 334–489 mya. The divergence times of the calibrated nodes were retrieved from the TimeTree website (<http://www.timetree.org/>). As shown in the phylogenetic tree, the estimated split time between *R. venosa* and *C. consors* was approximately 124.4 mya (Fig. 5).

Code availability

No custom code was used in this study. The data analyses used standard bioinformatic tools specified in the methods.

Received: 31 March 2023; Accepted: 9 August 2023;

Published online: 16 August 2023

References

- Ponder, W. F. & Lindberg, D. R. Towards a phylogeny of gastropod molluscs: an analysis using morphological characters. *Zool. J. Linn. Soc.* **119**, 83–265 (1997).
- Colgan, D. J., Ponder, W. F., Beacham, E. & Macaranas, J. Molecular phylogenetics of Caenogastropoda (Gastropoda: Mollusca). *Mol. Phylogenet. Evol.* **42**, 717–737 (2007).
- Barco, A. *et al.* A molecular phylogenetic framework for the Muricidae, a diverse family of carnivorous gastropods. *Mol. Phylogenet. Evol.* **56**, 1025–1039 (2010).
- Peng, C. *et al.* The first *Conus* genome assembly reveals a primary genetic central dogma of conopeptides in *C. betulinus*. *Cell Discov.* **7**, 11 (2021).
- Brauer, A. *et al.* The mitochondrial genome of the venomous cone snail *Conus consors*. *PLoS One* **7**, e51528 (2012).
- Mann, R. & Harding, J. M. Salinity tolerance of larval *Rapana venosa*: implications for dispersal and establishment of an invading predatory gastropod on the North American Atlantic coast. *Biol. Bull.* **204**, 96–103 (2003).
- Yang, M.-J. *et al.* Expression and activity of critical digestive enzymes during early larval development of the veined rapa whelk, *Rapana venosa* (Valenciennes, 1846). *Aquaculture* **519**, 734722 (2020).
- Harding, J. M. & Mann, R. Observations on the biology of the Veined Rapa whelk, *Rapana venosa* (Valenciennes, 1846) in the Chesapeake Bay. *J. Shellfish Res.* **18**, 9–17 (1999).
- Pastorino, G., Penchaszadeh, P. E., Schejter, L. & Bremec, C. *Rapana venosa* (Valenciennes, 1846) (Mollusca: Muricidae): A new gastropod in South Atlantic waters. *J. Shellfish Res.* **19**, 897–899 (2000).
- Harding, J. M. & Mann, R. Veined rapa whelk (*Rapana venosa*) range extensions in the Virginia waters of Chesapeake Bay, USA. *J. Shellfish Res.* **24**, 381–385 (2005).
- Lanfranconi, A., Brugnoli, E. & Muniz, P. Preliminary estimates of consumption rates of *Rapana venosa* (Gastropoda, Muricidae): a new threat to mollusk biodiversity in the Rio de la Plata. *Aquat. Invas.* **8**, 437–442 (2013).
- Mann, R., Harding, J. M. & Westcott, E. Occurrence of imposex and seasonal patterns of gametogenesis in the invading veined rapa whelk *Rapana venosa* from Chesapeake Bay, USA. *Mar. Ecol. Prog. Ser.* **310**, 129–138 (2006).
- Harding, J. M., Kingsley-Smith, P., Savini, D. & Mann, R. Comparison of predation signatures left by Atlantic oyster drills (*Urosalpinx cinerea* Say, Muricidae) and veined rapa whelks (*Rapana venosa* Valenciennes, Muricidae) in bivalve prey. *J. Exp. Mar. Biol. Ecol.* **352**, 1–11 (2007).
- Savini, D., Castellazzi, M., Favruzzo, M. & Occhipinti-Ambrogi, A. The alien mollusc *Rapana venosa* (Valenciennes, 1846; Gastropoda, Muricidae) in the northern Adriatic Sea: population structure and shell morphology. *Chem. Ecol.* **20**(sup1), 411–424 (2004).
- Shi, P. *et al.* Molecular response and developmental speculations in metamorphosis of the veined rapa whelk, *Rapana venosa*. *Integr. Zool.* **18**, 506–517 (2023).

16. Yang, M. J. *et al.* Symbiotic microbiome and metabolism profiles reveal the effects of induction by oysters on the metamorphosis of the carnivorous gastropod *Rapana venosa*. *Comput. Struct. Biotechnol. J.* **20**, 1–14 (2022).
17. Yang, M. J. *et al.* Integrated mRNA and miRNA transcriptomic analysis reveals the response of *Rapana venosa* to the metamorphic inducer (juvenile oysters). *Comput. Struct. Biotechnol. J.* **21**, 702–715 (2023).
18. Eid, J. *et al.* Real-time DNA sequencing from single polymerase molecules. *Science* **323**, 133–138 (2009).
19. Rao, S. S. P. *et al.* A 3D map of the human genome at kilobase resolution reveals principles of chromatin looping. *Cell* **159**, 1665–1680 (2014).
20. Ruan, J. & Li, H. Fast and accurate long-read assembly with wtdbg2. *Nat. Methods* **17**, 155–158 (2020).
21. Walker, B. J. *et al.* Pilon: an integrated tool for comprehensive microbial variant detection and genome assembly improvement. *PLoS One* **9**, e112963 (2014).
22. Song, H. *et al.* Genome survey on invasive veined rapa whelk (*Rapana venosa*) and development of microsatellite loci on large scale. *J. Genet.* **97**, e79–e86 (2018).
23. Zhang, G. *et al.* The oyster genome reveals stress adaptation and complexity of shell formation. *Nature* **490**, 49–54 (2012).
24. Bu, L. *et al.* Compatibility between snails and schistosomes: insights from new genetic resources, comparative genomics, and genetic mapping. *Commun. Biol.* **5**, 940 (2022).
25. Liu, C. *et al.* The genome of the golden apple snail *Pomacea canaliculata* provides insight into stress tolerance and invasive adaptation. *GigaScience* **7**, 9 (2018).
26. Liu, C. *et al.* Giant African snail genomes provide insights into molluscan whole-genome duplication and aquatic-terrestrial transition. *Mol. Ecol. Resour.* **21**, 478–494 (2021).
27. Albertin, C. B. *et al.* Genome and transcriptome mechanisms driving cephalopod evolution. *Nat. Commun.* **13**, 2427 (2022).
28. Waterhouse, R. M. *et al.* BUSCO applications from quality assessments to gene prediction and phylogenomics. *Mol. Biol. Evol.* **35**, 543–548 (2018).
29. Servant, N. *et al.* HiC-Pro: an optimized and flexible pipeline for Hi-C data processing. *Genome Biol.* **16**, 259 (2015).
30. Li, H. & Durbin, R. Fast and accurate long-read alignment with Burrows-Wheeler transform. *Bioinformatics* **26**, 589–595 (2010).
31. Wingett, S. *et al.* HiCUP: pipeline for mapping and processing Hi-C data. *F1000Res* **4**, 1310–1310 (2015).
32. Durand, N. C. *et al.* Juicer provides a one-click system for analyzing loop-resolution Hi-C experiments. *Cell Syst.* **3**, 95–98 (2016).
33. Dudchenko, O. *et al.* De novo assembly of the *Aedes aegypti* genome using Hi-C yields chromosome-length scaffolds. *Science* **356**, 92–95 (2017).
34. Durand, N. C. *et al.* Juicebox provides a visualization system for Hi-C contact maps with unlimited zoom. *Cell Syst.* **3**, 99–101 (2016).
35. Flynn, J. M. *et al.* RepeatModeler2 for automated genomic discovery of transposable element families. *Proc. Natl Acad. Sci. USA* **117**, 9451–9457 (2020).
36. Xu, Z. & Wang, H. LTR_FINDER: an efficient tool for the prediction of full-length LTR retrotransposons. *Nucleic Acids Res.* **35**, W265–W268 (2007).
37. Price, A. L., Jones, N. C. & Pevzner, P. A. De novo identification of repeat families in large genomes. *Bioinformatics* **21**(Supplement 1), i351–i358 (2005).
38. Chen, N. Using RepeatMasker to identify repetitive elements in genomic sequences. *Curr. Protoc. Bioinformatics* Chapter, Unit 4.10 (2004).
39. Bao, W., Kojima, K. K. & Kohany, O. Repbase Update, a database of repetitive elements in eukaryotic genomes. *Mob. DNA* **6**, 11 (2015).
40. Benson, G. Tandem repeats finder: a program to analyze DNA sequences. *Nucleic Acids Res.* **27**, 573–580 (1999).
41. Simakov, O. *et al.* Insights into bilaterian evolution from three spiralian genomes. *Nature* **493**, 526–531 (2013).
42. Knudsen, B., Kohn, A. B., Nahir, B., McFadden, C. S. & Moroz, L. L. Complete DNA sequence of the mitochondrial genome of the sea-slug, *Aplysia californica*: conservation of the gene order in Euthyneura. *Mol. Phylogenet. Evol.* **38**, 459–469 (2006).
43. Chen, Y., Ye, W., Zhang, Y. & Xu, Y. High speed BLASTn: an accelerated MegaBLAST search tool. *Nucleic Acids Res.* **43**, 7762–7768 (2015).
44. Lowe, T. M. & Chan, P. P. TRNAscan-SE On-line: integrating search and context for analysis of transfer RNA genes. *Nucleic Acids Res.* **44**, W54–W57 (2016).
45. Nawrocki, E. P. & Eddy, S. R. Infernal 1.1: 100-fold faster RNA homology searches. *Bioinformatics* **29**, 2933–2935 (2013).
46. Stanke, M. *et al.* AUGUSTUS: ab initio prediction of alternative transcripts. *Nucleic Acids Res.* **34**, W435–W439 (2006).
47. Kent, W. J. BLAT – The BLAST-like alignment tool. *Genome Res.* **12**, 656–664 (2002).
48. Doerks, T., Copley, R. R., Schultz, J., Ponting, C. P. & Bork, P. Systematic identification of novel protein domain families associated with nuclear functions. *Genome Res.* **12**, 47–56 (2002).
49. Kim, D., Langmead, B. & Salzberg, S. L. HISAT: a fast spliced aligner with low memory requirements. *Nat. Methods* **12**, 357–360–U121 (2015).
50. Pertea, M. *et al.* StringTie enables improved reconstruction of a transcriptome from RNA-seq reads. *Nat. Biotechnol.* **33**, 290–295 (2015).
51. Elsik, C. G. *et al.* Creating a honey bee consensus gene set. *Genome Biol.* **8**, R13 (2007).
52. NCBI sequence read archive. <https://identifiers.org/ncbi/insdc.sra:SRR22889214> (2022).
53. NCBI sequence read archive. <https://identifiers.org/ncbi/insdc.sra:SRR23517974> (2022).
54. NCBI sequence read archive. <https://identifiers.org/ncbi/insdc.sra:SRR23501451> (2022).
55. NCBI sequence read archive. <https://identifiers.org/ncbi/insdc.sra:SRR23501452> (2022).
56. NCBI sequence read archive. <https://identifiers.org/ncbi/insdc.sra:SRR23501453> (2022).
57. NCBI sequence read archive. <https://identifiers.org/ncbi/insdc.sra:SRR23501454> (2022).
58. Yang, M., Song, H. & Zhang, T. *Rapana venosa* breed wild species isolate MY-2022, whole genome shotgun sequencing project. *GenBank* <https://identifiers.org/ncbi/insdc:JAQIHA000000000> (2023).
59. Song, H. Annotations of *Rapana venosa* genome. *Figshare*. <https://doi.org/10.6084/m9.figshare.22362598.v1> (2023).
60. Laetsch, D. R. & Blaxter, M. L. BlobTools: Interrogation of genome assemblies. *F1000Res.* **6**, 1287 (2017).
61. Pardos-Blas, J. R. *et al.* The genome of the venomous snail *Lautoconus ventricosus* sheds light on the origin of conotoxin diversity. *GigaScience* **10**, giab037 (2021).
62. Harris, R. S. Improved Pairwise Alignment of Genomic DNA. Ph.D. dissertation, The Pennsylvania State University, Pennsylvania (2017).
63. Li, H. *et al.* TreeFam: a curated database of phylogenetic trees of animal gene families. *Nucleic Acids Res.* **34**, D572–D580 (2006).
64. Edgar, R. C. MUSCLE: multiple sequence alignment with high accuracy and high throughput. *Nucleic Acids Res.* **32**, 1792–1797 (2004).
65. Guindon, S. *et al.* New algorithms and methods to estimate maximum-likelihood phylogenies: assessing the performance of PhyML 3.0. *Syst. Biol.* **59**, 307–321 (2010).
66. Stamatakis, A. RAXML version 8: a tool for phylogenetic analysis and post-analysis of large phylogenies. *Bioinformatics* **30**, 1312–1313 (2014).
67. Huelsenbeck, J. P. & Ronquist, F. MrBayes: bayesian inference of phylogenetic trees. *Bioinformatics* **17**, 754–755 (2001).
68. Yang, Z. PAML 4: Phylogenetic analysis by maximum likelihood. *Mol. Biol. Evol.* **24**, 1586–1591 (2007).

Acknowledgements

This research was supported by the National Natural Science Foundation of China (Grant No. 32002409, 42206086, 31972814, and 32002374), the China Agriculture Research System of MOF and MARA, and the Creative Team Project of the Laboratory for Marine Ecology and Environmental Science, Qingdao National for Marine Science and Technology (Grant No. LMEESCTSP-2018). Hao Song was supported by the Young Elite Scientists Sponsorship Program by CAST (Grant No. 2021QNRC001) and Youth Innovation Promotion Association by CAS. The funders had no role in the study design, data collection and analysis, decision to publish, or preparation of the manuscript. We thank Oceanographic Data Center, IOCAS for support of data analysis.

Author contributions

The authors' contributions to specific working groups are indicated below. H. Song: steering committee, genome sequencing, genome assembly, genome annotation, data processing, statistical analysis, and manuscript writing. T. Zhang: steering committee. M. Yang: sampling, genome sequencing, genome assembly, genome annotation, data processing, statistical analysis, and manuscript writing. Z. Yu: sampling. Z. Hu: sampling. C. Zhou: sampling. P. Hu: sampling. P. Shi: genome sequencing, genome assembly, genome annotation, data processing, and statistical analysis. Z. Li: data processing and statistical analysis, manuscript writing. All authors have read and approved the final manuscript.

Competing interests

The authors declare no competing interests.

Additional information

Correspondence and requests for materials should be addressed to T.Z.

Reprints and permissions information is available at www.nature.com/reprints.

Publisher's note Springer Nature remains neutral with regard to jurisdictional claims in published maps and institutional affiliations.



Open Access This article is licensed under a Creative Commons Attribution 4.0 International License, which permits use, sharing, adaptation, distribution and reproduction in any medium or format, as long as you give appropriate credit to the original author(s) and the source, provide a link to the Creative Commons licence, and indicate if changes were made. The images or other third party material in this article are included in the article's Creative Commons licence, unless indicated otherwise in a credit line to the material. If material is not included in the article's Creative Commons licence and your intended use is not permitted by statutory regulation or exceeds the permitted use, you will need to obtain permission directly from the copyright holder. To view a copy of this licence, visit <http://creativecommons.org/licenses/by/4.0/>.

© The Author(s) 2023